Deep acceptor states of platinum and iridium in 4*H*-silicon carbide

J. Grillenberger,* U. Grossner, and B. G. Svensson
Department of Physics, University of Oslo, P. O. Box 1048, Blindern, N-0316 Oslo, Norway

F. Albrecht and W. Witthuhn
Institut für Festkörperphysik, Friedrich-Schiller-Universität Jena, Max-Wien-Platz 1, D-07743 Jena, Germany

R. Sielemann
Hahn-Meitner-Institut Berlin, Glienicker Straße 100, D-14109 Berlin, Germany
(Received 10 May 2004; published 15 November 2004)

Band gap states of platinum and iridium in the hexagonal polytype 4*H* of silicon carbide are investigated by means of deep level transient spectroscopy (DLTS) in *n*- as well as *p*-type epitaxial layers. To establish a definite chemical assignment of band gap states to Pt and Ir the radioactive isotope ^{188}Pt was incorporated into 4*H*-SiC samples by recoil implantation. During the nuclear decay of ^{188}Pt via the unstable ^{188}Ir to the stable ^{188}Os, the concentration of band gap states is traced by DLTS whereby characteristic concentration changes lead to an unambiguous assignment of two band gap states to ^{188}Pt. The two levels are interpreted as one Pt-related defect structure with two different charge states in the band gap of 4*H*-SiC: a double-negative acceptor at 0.81 eV and a single-negative acceptor at 1.47 eV below the conduction band edge E_C. Iridium was found to generate one acceptorlike state ($E_C-0.82$ eV) in the band gap of 4*H*-SiC. Further, acceptor states at $E_C-0.31$ eV, $E_C-0.41$ eV, $E_C-0.50$ eV and donor states at $E_V+0.60$ eV, $E_V+0.90$ eV, $E_V+1.09$ eV (E_V is the valence band edge) are preliminarily assigned to defects involving osmium. It was found that recoil processes taking place during the nuclear decay may generate different complex structures related to Os. Therefore, the assignment to specific Os structures is not definite. The deep acceptor state of platinum is considered an interesting candidate for a compensating center close to the midgap position in 4*H*-SiC in order to produce semi-insulating SiC layers and control carrier lifetimes.

DOI: 10.1103/PhysRevB.70.205209 PACS number(s): 71.55.Ht, 72.20.Jv, 23.20.Lv

I. INTRODUCTION

Silicon carbide (SiC) is a wide-band-gap semiconductor (E_{gap} between 2.3 eV and 3.3 eV) which is expected to replace conventional semiconductors like Si and GaAs in high-power, high-frequency, high-temperature applications. It occurs in more than 200 different crystal structures, so-called polytypes, of which each exhibits a characteristic band gap. Intrinsic defects and impurities in the crystal are known to give rise to energy levels in the band gap and are, therefore, crucial for the functionality of any semiconductor device. Consequently, it is crucial to establish a correlation between band gap states and certain defect structures. Especially, there is a general continuous interest in compensating centers at or close to the midgap position of SiC in order to produce semi-insulating layers for high-frequency devices. In silicon carbide the most prominent impurity intentionally introduced into the crystal to control the carrier lifetime is vanadium.[1,2] In addition to this element, the deep acceptor state of tungsten was proposed to act as a deep compensating center in SiC.[3] In the case of the traditional semiconductor Si among other elements, platinum is known to have a midgap state responsible for recombination processes.[4–8] Hence, this study is directed to the investigation of deep levels of Pt in 4*H*-SiC and it will be shown that Pt, if introduced into 4*H*-SiC crystals, will lead to two deep acceptorlike levels in the band gap and, indeed, to an acceptor state close to the midgap position which may serve as an efficient compensating center.

Band gap states in 4*H*-SiC were characterized by means of deep level transient spectroscopy (DLTS) with respect to activation energy E_T and capture cross section σ. Though this technique is very sensitive to the concentration of a trap, it does not reveal *a priori* its chemical or structural nature. To circumvent this deficiency the features of the radiotracer technique were utilized: instead of stable impurity atoms the radioactive isotope ^{188}Pt was incorporated. It decays with its well known half-life of $T_{1/2}=10.2$ days to ^{188}Ir which further decays to the stable ^{188}Os with $T_{1/2}=1.7$ days.[9] The decisive advantage of combining conventional semiconductor spectroscopy with the radiotracer concept is given by the nuclear decay of the deployed radioactive isotope. It provides an element-specific signal which allows a definite correlation between the respective radioactive isotope and concentration changes, observed by an appropriate spectroscopic method, which is DLTS in this case. Reviews of the radiotracer DLTS technique can be found in Refs. 10 and 11.

In the course of this study band gap states were assigned to Pt, Ir, and tentatively to Os. Furthermore, the generation of electrically active defects induced by recoil processes taking place during the nuclear decay is observed.

To confirm the studies on radioactive isotopes and to carry out further detailed DLTS studies stable isotopes of the elements Pt and Ir were also implanted in a collateral experiment.

II. EXPERIMENTAL DETAILS

To electrically characterize Pt-related band gap states the experiments were carried out using *n*- and *p*-type 4*H*-SiC epitaxial layers grown on heavily doped substrates ($\sim 10^{19}$). The net shallow doping concentration was determined by capacitance-voltage profiling to be in the range of $(1-6)\times 10^{15}$ cm^{-3} for *n*-type samples (dopant N) and $(3-6)\times 10^{15}$ cm^{-3} for *p*-type samples (dopants B, Al), respectively. The radioactive isotopes were introduced by recoil implantation[12] at the Ionen-Strahl-Labor (ISL) of the Hahn-Meitner-Institut in Berlin, Germany, whereas stable Pt and Ir were incorporated into the samples by ion implantation at the tandetron accelerator JULIA in Jena, Germany. During every implantation procedure a part of the samples was covered with aluminum foil to retain an unimplanted reference.

A. Radioactive isotopes

The tracer atom employed is the radioactive isotope ^{188}Pt which decays to ^{188}Ir with a half-life of $T_{1/2}=10.2$ days. The isotope ^{188}Ir is unstable itself and further decays to the stable ^{188}Os with a half-life of 1.7 days.[9]

To obtain ^{188}Pt, a ^{12}C primary beam of 90 MeV kinetic energy was led on a ^{181}Ta target foil (thickness ~ 1 μm) in order to induce nuclear reactions. The compound nucleus ^{193}Au formed by the fusion of ^{12}C and ^{181}Ta immediately emits five nucleons (preferentially neutrons) and ends up as the neutron-deficient ^{188}Au which decays with a comparatively short half-life of just 9 min and, therefore, saturates the desired state ^{188}Pt.

As a feature of the compound nuclear reaction, other isotopes of the same mass number $A=188$ and also mass numbers adjacent to that (i.e., $A=187$ and $A=189$) are coimplanted in addition to ^{188}Pt. Thus, the samples implanted with radioactive isotopes were investigated with γ-ray spectroscopy to reveal the mixture and amount of implanted isotopes and to monitor the loss of the ^{188}Pt isotopes during sample preparation. According to γ-ray spectroscopy the initial amount of implanted ^{188}Pt atoms in each sample was 9.0×10^{8} which corresponds to an implantation dose of 1.5×10^{10} cm^{-2} for ^{188}Pt. It was found that ^{189}Ir ($T_{1/2}=13.2$ days) and ^{188}Ir($T_{1/2}=1.7$ days) are also relevant for the present experiments and that other isotopes are negligible in number or have a half-life not relevant on the time scale of this experiment. All isotopes found in the samples by means of γ-ray spectroscopy are listed in Table I with their half-lives and their implanted concentrations.

The implantation energy of the radioactive isotopes results from the recoil imposed on the reaction products: the atoms are kicked out of the target foil with an energy of about 5–6 MeV with a broad distribution to lower energies. The samples to be implanted are mounted off axis to the primary ^{12}C beam behind the target foil and are, thus, implanted with the recoiling reaction products and, inevitably, also with stable Ta atoms kicked out of the target foil without nuclear transformation. This implantation technique leads to a widespread distribution of the atoms within the samples to a maximum depth of 1 μm as calculated with the TRIM code.[13] Considering these facts, the implantation dose for the isotopes can be converted to a concentration which is measured by means of DLTS. Assuming a roughly homogeneous implantation profile to a maximum depth of 1 μm, concentrations of 1.5×10^{14} cm^{-3} are obtained for ^{188}Pt and 6×10^{13} cm^{-3} for ^{189}Ir, respectively.

TABLE I. Isotopes found in the SiC samples recoil implanted with ^{188}Pt. The total amount of each isotope is dated back to the end of the implantation. The given concentrations were calculated assuming a roughly homogeneous implantation to a maximum depth of 1 μm.

Isotope	Half-life (days)	Total number (10^8)	Concentration (10^{13} cm^{-3})
^{186}Ir	0.69	0.1	0.2
^{187}Ir	0.44	1.2	2.0
^{188}Ir	1.73	2.0	3.3
^{188}Pt	10.2	9.0	15
^{189}Ir	13.2	3.8	6.0

B. Ion implantation of stable isotopes

In a supplementary experiment stable isotopes of Pt and Ir were implanted at the tandetron ion accelerator JULIA of the University of Jena. To achieve a fairly homogeneous impurity concentration of about 2×10^{14} cm^{-3} in a depth between 0.2 and 1.0 μm, fourfold implantations of each element with implantation energies ranging between 1.0 and 5.2 MeV were performed. The implantation dose used at each energy was between 4 and 12×10^{9} cm^{-2} as determined with the TRIM code.[13]

C. Annealing and diode preparation

To restore the crystal structure and to electrically activate the implanted impurities, after each implant the samples were annealed at 1900 K for 5 min in sealed quartz ampoules filled with argon. Subsequently, they were oxidized in pure O_2 at 1600 K for 30 min. After removing the resulting oxide layer (thickness ~ 150 nm) by etching the samples in hydrofluoric acid for 5 min, circular Schottky contacts of 0.5 mm diameter were produced by evaporating Ni on top of the epitaxial layers. The Ohmic contact was obtained by evaporating Ti on the entire backside (the highly doped substrate) of the samples. Before annealing and after diode preparation each sample was investigated with γ-ray spectroscopy which revealed that an amount of 5–10 % of ^{188}Pt was lost during the annealing and diode preparation, presumably caused by the etching of the sacrificial oxide layer.

D. Electrical characterization

The DLTS measurements were carried out in a setup described elsewhere.[14] Spectra were recorded in temperature ranges between 650 K and 40 K (*n* type) and 650 K and 200 K (*p* type) with a temperature rate of 4 K/min from the higher to the lower temperature. Capacitance transients were

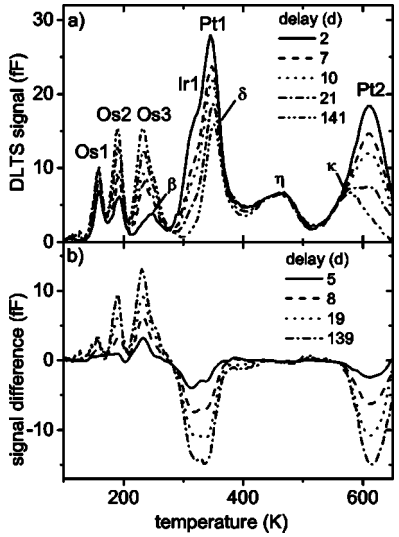

FIG. 1. (a) DLTS spectra recorded several times on an *n*-type 4*H*-SiC sample implanted with ^{188}Pt. The spectra correspond to emission rates of $(0.85\ \mathrm{s})^{-1}$. (b) Difference spectra obtained by subtracting the initial spectrum from the sequencing spectra recorded during the ^{188}Pt decay.

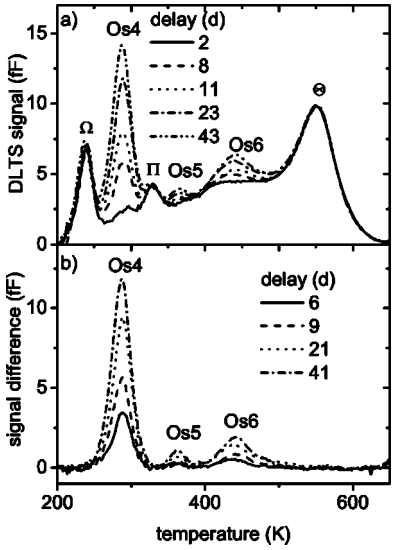

FIG. 2. (a) DLTS spectra recorded several times on a *p*-type 4*H*-SiC sample implanted with ^{188}Pt. Rate window: $(45\ \mathrm{ms}^{-1})$. (b) Difference spectra calculated from (a). No decreasing signals are detectable in *p*-type material.

measured within three predefined time windows (5 ms, 100 ms, and 2 s), digitized, and processed with a computer. In this manner emission rates between $(1\ \mathrm{ms})^{-1}$ and $(1.5\ \mathrm{s})^{-1}$ could be filtered from the capacitance transients. Unless otherwise stated, the reverse bias U_R was set to −15 V or +15 V on *n*- or *p*-type samples, respectively, to ensure detection over the full implantation width. To fill traps with charge carriers, the reverse bias was reduced to zero volts ($U_P = 0$ V) for 1 ms.

In the present study, DLTS parameters of any trap are given assuming a temperature-independent apparent capture cross section σ_a. The correction of the trap energy E_T for a possible temperature dependence of σ_a can easily be performed by adding nkT (for T^{-n}, $n=2$–3). For the traps assigned to Pt and Ir, the filling pulse width t_p was varied between 10 ns and 10 ms in order to reveal the capture kinetics of these deep levels. The DLTS signal dependence on the pulse width was evaluated according to Pons[15] to obtain the true capture cross section σ_m. However, for the samples used the capture process was always faster than the minimum available pulse length, and thus the evaluated σ_m values have to be regarded as a lower limit.

In addition, to investigate the dependence of the emission time constant on the electric field strength (Poole-Frenkel effect) the electric field strength that the traps are exposed to during carrier emission was varied in a manner which is commonly referred to as the *double-correlation DLTS method* in the literature (see, e.g., Ref. 16).

III. RESULTS AND DISCUSSION

DLTS spectra of the samples implanted with the radioactive isotope ^{188}Pt were recorded several times on *n*-type [Fig. 1(a)] as well as *p*-type [Fig. 2(a)] samples during the nuclear decay. Clearly, time-dependent DLTS signals can be detected in the spectra recorded on both the conducting types whereas the *p*-type samples were exclusively dominated by signals increasing in concentration. In almost every case the DLTS peaks are either superimposed by time-stable signals or exhibit a broadening if compared to the theoretical DLTS peak shape. It is crucial for a standard DLTS parameter evaluation that the exact temperature position of a peak is known for an accurate Arrhenius evaluation.[17] Utilizing the fact that the DLTS spectra are highly reproducible for constant trap concentrations, for each specimen the initial DLTS spectrum was subtracted from all the spectra recorded subsequently in the course of the nuclear decay. DLTS signals not subject to the decay of ^{188}Pt, i.e., signals stable in time, are, thus, eliminated and the number of peaks is limited to signals related to traps with time-dependent concentration [Fig. 1(b) for *n*-type samples and Fig. 2(b) for *p*-type samples]. This approach is justified, as the DLTS signal is directly proportional to the trap concentration N_t provided that N_t is much smaller than the shallow doping concentration N_s ($N_t \ll N_s$). Hence, traps with decreasing concentration will turn out as negative peaks increasing in amplitude, whereas traps with increasing concentration will exhibit positive peaks also increasing in amplitude. In this manner, not only can band gap states correlating with the nuclear decay chain be uniquely distinguished from stable states resulting from electrically active defects caused by irradiation, but also the accuracy of the Arrhenius evaluation of deep level parameters is improved as the time-dependent peaks are isolated from constant overlapping signals.

First, decreasing peaks will be discussed and then increasing signals are treated. Finally, attention is drawn to band gap states not subject to the radioactive decay, i.e., stable signals.

A. Traps of decreasing concentration

Deep levels with decreasing concentration were exclusively found in the *n*-type samples. In this section we will

TABLE II. Deep level parameters and interpretation of band gap states of time-dependent concentration. The capture cross section σ_m is given as an upper limit as the shallow doping concentration was too high for accurate capture kinetics measurements. The assignment and interpretation of Os1–Os6 to osmium are preliminary.

Label	Energy (eV)	σ_a (10^{-15} cm^2)	σ_m (10^{-16} cm^2)	Interpretation
Ir1	$E_C-0.82(2)$	70	>4	Ir (0/−)
Pt1	$E_C-0.81(2)$	4	>1	Pt (−/−−)
Pt2	$E_C-1.46(4)$	3	>1	Pt (0/−)
Os1	$E_C-0.31(2)$	0.4		Os (0/−)
Os2	$E_C-0.41(2)$	1		Os (0/−)
Os3	$E_C-0.50(2)$	0.5		Os+defect (0/−)
Os4	$E_V+0.60(2)$	0.5		Os+defect (+/0)
Os5	$E_V+0.92(2)$	30		Os (+/0)
Os6	$E_V+1.09(3)$	9		Os (+/0)

show that these band gap states are associated with Pt and Ir. The difference spectra obtained from the *n*-type samples [Fig. 1(b)] exhibit a broad signal in the temperature range between 280 K and 380 K consisting of two overlapping peaks (labeled Ir1 and Pt1) and one broad decreasing peak at 614 K labeled Pt2. The difference spectra were deduced for several rate windows to establish a more precise determination of the energy positions of Ir1, Pt1, and Pt2. The deep level parameters calculated from the difference spectra are given in Table II. The difference signal Pt2 and, thus, the concentration of the corresponding trap decreases exponentially with a time dependence reflecting the half-life $T_{1/2}$ = 10.2 days of the nuclear decay of ^{188}Pt [Fig. 3(a)]. The correspondence between the nuclear decay of ^{188}Pt and the decrease of the trap concentration with time unambiguously assigns Pt2 to a defect structure containing one Pt atom. For the two overlapping peaks Ir1 and Pt1 the situation is more complex. In order to clarify the structure of these signals DLTS spectra corresponding to an emission rate of $(12.5\ \text{ms})^{-1}$ are presented [Fig. 4(a)]. Here, the broad DLTS signal Ir1/Pt1 can be further resolved, facilitating a more accurate evaluation of the concentration changes. A least squares fit of an exponential function representing a single nuclear decay reveals a half-life of 10 ± 1 days for Pt1, which corresponds well to the ^{188}Pt decay. However, for Ir1 fitting a function representing a single exponential decay to the peak height versus time data [Fig. 4(b)] a half-life of 12 ± 2 days is obtained. Within errors this value still roughly corresponds with the half-life of ^{188}Pt. However, it is furthermore observed that the amplitude of the decrease of Ir1 is a factor of 1.5 smaller than that of Pt1. Especially the latter fact is a strong hint that the band gap state Ir1 does not correspond to ^{188}Pt. In the following it will be shown that Ir1 corresponds to a defect structure containing one Ir atom and Pt1 to a defect structure containing one Pt atom.

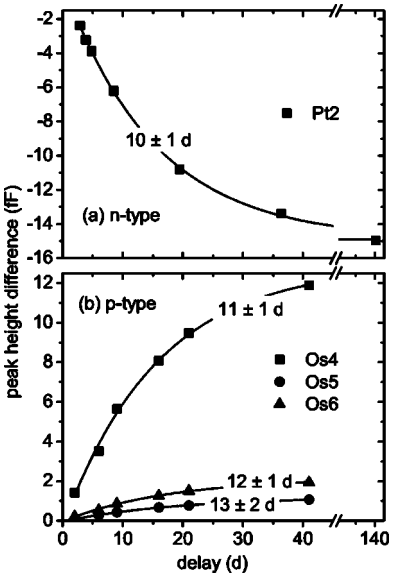

FIG. 3. (a) Peak height versus time of Pt2 found in *n*-type material. It decreases with delay time reflecting the half-life of ^{188}Pt of 10.2 days. The data refer to the difference spectra shown in Fig. 1(b). (b) displays the peak height versus delay time for peaks found in *p*-type samples. For clarity, the other time-dependent traps found in *n*-type 4*H*-SiC are treated in Fig. 4.

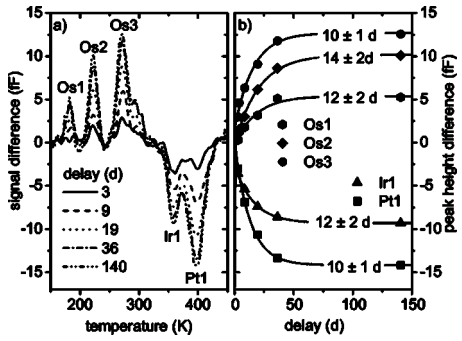

FIG. 4. (a) Difference spectra extracted from DLTS measurements on *n*-type samples corresponding to emission rates of $(12.5\ \text{ms})^{-1}$. This results in a higher resolution and the peaks Ir1 and Pt1 were further resolved. In these high-resolution spectra the different time behavior of Ir1 and Pt1 becomes obvious. Clearly, Ir1 and Pt1 represent deep levels resulting from different electrically active defects. (b) Peak height versus time data. The solid lines are exponential functions fitted to the peak height data taken from (a).

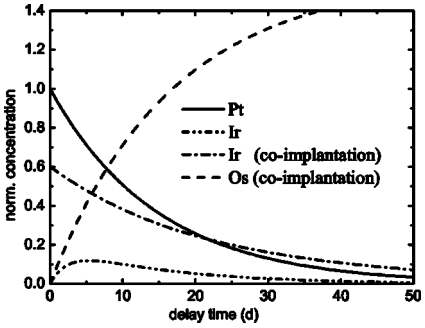

FIG. 5. Theoretical concentration course of Pt, Ir, and Os. Due to non-negligible coimplantation of ^{189}Ir and ^{188}Ir the true Ir (dash-dotted line) and Os (dashed line) concentrations deviate from simple exponential behavior. The curves were calculated for an isotope mixture as determined in Table I and are normalized to the initial implanted ^{188}Pt concentration.

As outlined in Sec. II A, ^{188}Pt decays to ^{188}Ir with a half-life of 10.2 days. The isotope ^{188}Ir itself is unstable and decays to the stable ^{188}Os with a half-life of 1.7 days, which is approximately 17% of the half-life of ^{188}Pt. Thus, the state ^{188}Ir is continuously fed by the transmutation of ^{188}Pt but decays relatively fast to ^{188}Os. If only ^{188}Pt were present in the samples after recoil implantation, the concentration of the corresponding Ir-related band gap state would behave as denoted in Fig. 5 by the double-dot-dashed curve. According to the given half-lives there would be a saturation (maximum) of the ^{188}Ir concentration about 5 days after the ^{188}Pt implantation, but because of the sample preparation lasting about 40 h and the ^{188}Pt decay taking place already during the implantation procedure (duration $\sim$24 h), it is not possible to observe the saturation of Ir. In addition to the feeding of the ^{188}Ir state by ^{188}Pt, ^{189}Ir (and some ^{188}Ir) is also coimplanted in a non-negligible amount (see Table I), as determined by γ-ray spectroscopy. Taking both these facts into account, the feeding of Ir and its coimplantation, the theoretical behavior of the iridium concentration deviates from a single-exponential behavior. The dash-dotted curve in Fig. 5 demonstrates the Ir concentration versus time in samples implanted with an isotope mixture as listed in Table I. A fit of a function representing a single exponential decay to such a concentration course leads to an *apparent* half-life of 13 days. This is in close agreement with the value obtained for the half-life of Ir1. Hence, Ir1 is assigned to a defect which involves one Ir atom, whereas Pt1 corresponds to a structure containing one Pt atom. These conclusions will be further confirmed in Sec. III C while discussing the samples implanted with stable Pt and Ir isotopes.

B. Increasing signals

In the *n*-type samples a set of three rising DLTS peaks Os1, Os2, and Os3 is detected in the temperature range between 100 K and 300 K (Fig. 1 and 4). These three peaks correspond to deep levels located at 0.31 eV ($\sigma_a = 4\times10^{-16}$ cm^2), 0.41 eV ($\sigma_a = 1\times10^{-15}$ cm^2), and 0.50 eV ($\sigma_a = 5\times10^{-16}$ cm^2) below E_c. A straightforward interpretation of Os1–Os3 would be to assign them to the final product of the nuclear decay, i.e., ^{188}Os. However, radioactive isotopes may in the course of their decay be subject to recoil processes which are capable of forming probe-related defects, e.g., a vacancy and an interstitial atom, as the impurity atom is kicked from its initial location in the lattice.[18,19] These recoil effects can be initiated by an emitted γ ray, neutrino ν, or charged particle that may generate defects correlated to the tracer probe. Within the decay scheme of ^{188}Pt, the energy difference Q_{EC} of the 0^+ state of ^{188}Pt and the ground state of ^{188}Ir is 507 keV.[9] The dominating decay path is the electron capture with an abundance of 47% with energies of 312 keV and 195 keV of the emitted neutrino and γ ray, respectively. As $E_{\nu,\gamma}=p_{\nu,\gamma}c$ holds, the recoil energy E_R imposed on ^{188}Ir by the emission of a γ ray or neutrino ν can be calculated from the transferred momentum $p_{\gamma,\nu}$:

$$E_R = \frac{p_{\gamma,\nu}^2}{2M} = \frac{E_{\gamma,\nu}^2}{2Mc^2}, \tag{1}$$

where c is the speed of light and M the mass of the ^{188}Ir nucleus. Therefore, along with the decay of ^{188}Pt to ^{188}Ir a maximum recoil energy of only 0.28 eV is imposed on the nucleus through the emission of a neutrino. If this value is compared to the displacement energy threshold, which is estimated to be in the range[20] between 13 eV and 30 eV in SiC it appears unlikely that ^{188}Ir is kicked from its position in the lattice or that other defects are formed. In contrast, the decay from ^{188}Ir to ^{188}Os takes place with an energy difference of $Q_{EC}=2809$ keV whereby large fractions of γ rays with at least 2.2 MeV are emitted.[9] This corresponds to a recoil energy of 15 eV which is of the order of the displacement energy threshold and, in addition, impurity atoms are anticipated to have a smaller displacement energy than the host atoms. Therefore, the generation of more complex defect structures during the nuclear decay cannot be excluded. On the other hand the decay of the coimplanted ^{189}Ir takes place with an energy difference Q_{EC} of 532 keV leading to a maximum recoil of just 0.8 eV imposed on the nucleus. Hence, a displacement of the atoms is not expected from this decay. As osmium could not be implanted as a stable isotope an exact interpretation for the defects arising in the *n*- and *p*-type samples during the nuclear decay is not possible. Further studies covering this subject in detail are in progress.[21] At this stage the assignment of the band gap states Os1–Os6 to osmium is preliminary: the concentration increase of Os3 and Os4 exhibits a close agreement with the half-life of the ^{188}Pt decay and an assignment of Os3 and Os4 to a complex containing one Os atom resulting from the ^{188}Pt decay appears to be plausible. Due to the recoil of 15 eV imposed on the daughter atom ^{188}Os, Os3 and Os4 are most likely due to an Os atom which was displaced from the site where the ^{188}Pt atoms were residing after implantation and subsequent annealing. The defects Os1,Os2, and Os5,Os6 on the other hand may result from the decay of coimplanted isotopes to ^{189}Os. In this case, the maximum recoil energy is only 0.8 eV and a displacement is not expected. This is also an indication that these levels are due an isolated (substitutional) Os atom though the involvement of other defects (intrinsic or extrinsic) cannot be excluded. Further evidence in

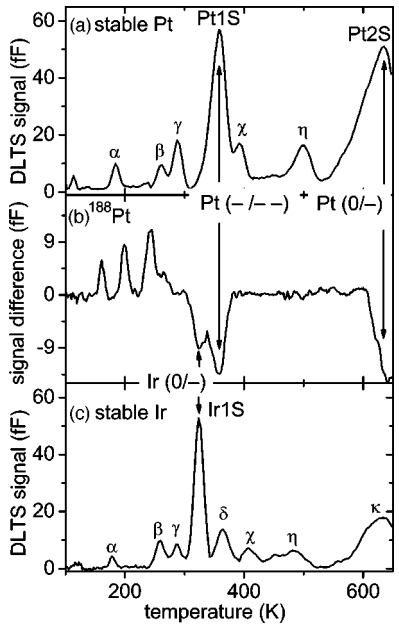

FIG. 6. DLTS spectra recorded on *n*-type 4*H*-SiC implanted with stable (a) Pt and (c) Ir. (b) shows a difference spectrum obtained from a sample implanted with radioactive ^{188}Pt. The arrows clarify the match of the radiotracer and the stable experiments.

favor of the latter conclusions is given by the half-lives obtained for the concentrations of these presumably Os-related defects: Os3 and Os4 appear with the half-life of 10 days determined by the ^{188}Pt decay whereas Os1,Os2, and Os5, Os6 increase with half-lives close to that of ^{189}Ir (13.2 days). Consequently, there must exist at least two different electrically active defect structures related to the formation of Os, i.e., one resulting from the ^{188}Ir transmutation to Os and one from the transmutation of ^{189}Ir to Os, which each obviously lead to band gap states. Whether each decay chain produces only one defect structure leading to deep levels of different charge states (no Poole-Frenkel effect was observed for either trap) cannot be unambiguously decided.

C. Stable isotopes

The DLTS spectra of the samples implanted with stable Pt [Fig. 6(a)] exhibit two dominating peaks labeled Pt1*S* and Pt2*S* (the letter *S* denotes the implantation of stable elements). According to the standard DLTS evaluation, Pt1*S* and Pt2*S* can be described by a thermal activation energy of 0.83 (3) eV and 1.48 (6) eV, respectively. These values are in good agreement with that of Pt1 and Pt2 derived from the radiotracer experiment. Consequently, the conclusions drawn from the radiotracer experiments are confirmed and Pt1*S* and Pt2*S* are conclusively assigned to Pt. In this context it is pointed out that the deep level parameters derived from the radiotracer experiments are more accurate than those from the stable implants due to the elimination of underlaying stable defects not corresponding to platinum. The same criteria apply for the DLTS spectra recorded on the samples implanted with stable Ir [Fig. 6(c)]. Here, one dominating peak Ir1*S* is observed corresponding to an activation energy of 0.82 eV and an apparent capture cross section σ_a of 8×10^{-14} cm^2 which very well correspond to the parameters obtained for the Ir-related level Ir1. Comparing Fig. 6(b), showing the difference spectrum obtained from the radiotracer experiment, with the spectra recorded on the samples implanted with [Fig. 6(a)] stable Pt and [Fig. 6(c)] stable Ir, the close correlation between the two types of experiments becomes obvious.

The electrical activation of the implanted stable Pt and Ir atoms was derived from the DLTS spectra shown in Fig. 6. The concentration of the Pt-related levels Pt1*S* and Pt2*S* is in the range of $(1.5-2) \times 10^{14}$ cm^{-3}, which is in close agreement with the nominally implanted platinum concentration of 2×10^{14} cm^{-3}. For the Ir-related level Ir1*S* a concentration of $(1-1.5) \times 10^{14}$ cm^{-3} is obtained, which is slightly less than the concentration of implanted iridium. Taking into account systematic errors of 50% for absolute concentrations derived from DLTS measurements and uncertainties in the determination of small implantation doses, the difference is not remarkable. The high degree of electrical activation of the implanted Pt of more than 50% is not only evidence for the correct assignment of Pt1*S* and Pt2*S* to one and the same defect structure containing one Pt atom but also a strong indication that the impurity atoms reside on substitutional lattice sites, presumably Si sites. The latter also applies for Ir1*S* which is most likely due to a substitutional Ir atom residing on a Si site.

D. Influence of the electrical field strength

The electric field dependence of the emission time constants (Poole-Frenkel effect) of the Pt- and Ir-related traps was investigated. This was done at constant temperatures in a manner to keep the probed part of the depletion region constant and as small as possible, i.e., to minimize the error in the mean electric field applied.[22] The method is commonly referred to as double-correlation DLTS (see, e.g., Ref. 16). The variation of the electric field strength F from 50 ± 20 kV/cm to 150 ± 30 kV/cm revealed no significant field enhancement of the carrier emission either from the Ir-related trap Ir1 or the Pt-related traps Pt1 and Pt2. Hence, there is no field-induced barrier lowering of a Coulomb center which could be interpreted as a donorlike state according to the Poole-Frenkel effect. Therefore, the centers Ir1, Pt1, and Pt2 are interpreted to be acceptorlike, whereas the centers Pt1 and Pt2 are most likely due to the same defect structure (containing one Pt atom) leading to a double-negative (Pt1) and single-negative (Pt2) acceptor state in the band gap.

E. Defects not related to the nuclear decay

Deep levels not related to the nuclear decay, i.e., signals stable with respect to time, are labeled with greek letters. Their trap parameters (see Table III) are compared with DLTS signatures of deep levels found during other DLTS studies under similar experimental conditions. This comparison mainly refers to experiments treating defects induced by irradiation, i.e., complexes involving intrinsic defects. No

TABLE III. Deep level parameters of band gap states not related to either Pt, Ir, or Os. Those defects and/or impurities cannot be identified unambiguously but are compared to energy states already found in other studies dealing with experimental conditions comparable to ours. The last column gives the reference with the defect name the authors used.

Label	Energy (eV)	σ_a (10^{-15} cm^2)	Related defects (reference)
α	$E_C-0.19(2)$	1	P_3
β	$E_C-0.58(3)$	10	ID9 (23), 0.62 eV (24)
γ	$E_C-0.68(3)$	70	Z_1/Z_2 (25), Z_1 (23), EH_2 (26), 0.68 eV (24)
δ	$E_C-0.85(3)$	6	RD_1 (23)
χ	$E_C-0.95(3)$	10	RD_2 (23)
η	$E_C-1.1(4)$	0.5	RD_3 (23)
κ	$E_C-1.5(1)$	8	EH6/EH7 (27)
Ω	$E_V+0.51(2)$	0.8	
Π	$E_V+0.77(3)$	5	
Θ	$E_V+1.4(1)$	3	

studies on intrinsic defects in *p*-type 4*H*-SiC are reported in the literature.

IV. CONCLUSION

DLTS investigations were performed on *n*- as well as *p*-type 4*H*-SiC samples implanted with either radioactive ^{188}Pt or stable Pt. Band gap states of time-dependent concentrations have been observed in both conducting types, but the *p*-type samples exhibit only arising deep levels. A definite chemical assignment of band gap states originating from Pt and Ir was obtained: Pt has one double acceptor state Pt1 located at $E_C-0.81(2)$ eV and a remarkable single acceptor state Pt2 close to midgap at $E_C-1.46(4)$ eV. The deep acceptor state of Pt is, besides vanadium, the deepest impurity-related center in 4*H*-SiC identified up to now, and very suitable for the accomplishment of semi-insulating SiC. No Pt-related defect was found in the lower part of the band gap observed with an uncertainty of 5% of the total Pt concentration ($\sim 2\times 10^{14}$ cm^{-3}).

In the case of Ir, one acceptorlike state Ir1 at $E_C-0.82$ eV was observed and unambiguously identified to involve one Ir atom.

A set of three growing levels was found in both *n*- and *p*-type samples, i.e., six deep levels emerge during the decay of ^{188}Pt. The two levels Os3 and Os4 located at $E_C-0.41(2)$ eV and $E_V+0.60(2)$ eV are tentatively assigned to a defect containing one Os atom resulting from the transmutation of ^{188}Ir to ^{188}Os and are most likely associated with recoil effects taking place. The traps Os1 at $E_C-0.15(2)$ eV, Os2 at $E_C-0.31(2)$ eV, Os5 at $E_V+0.92(2)$ eV, and Os6 at $E_V+1.09(3)$ eV are assigned to Os-related defects of a structure different from the latter. In this case no recoil effects are expected and the probe atoms should remain on their lattice sites, presumably substitutional on Si sites. The exact structure of the Os-related defects is the subject of a further study.[21]

ACKNOWLEDGMENTS

Financial support by the Norwegian Research Council and the FUNMAT program at the University of Oslo is highly appreciated.

*Electronic address: j.k.grillenberger@fys.uio.no

[1] H. M. Hobgood, R. C. Glass, G. Augustine, R. H. Hopkins, J. Jenny, M. Skowronski, W. C. Mitchel, and M. Roth, Appl. Phys. Lett. **66**, 1364 (1995).
[2] J. R. Jenny, M. Skowronski, W. C. Mitchel, H. M. Hobgood, R. C. Glass, G. Augustine, and R. H. Hopkins, J. Appl. Phys. **73**, 726 (1995).
[3] N. Achtziger, G. Pasold, R. Sielemann, C. Hülsen, J. Grillenberger, and W. Witthuhn, Phys. Rev. B **62**, 12 888 (2000).
[4] K. P. Lisiak and A. G. Milnes, J. Appl. Phys. **46**, 5229 (1975).
[5] S. J. Pearton and E. E. Haller, J. Appl. Phys. **54**, 3613 (1983).
[6] W. Stoffier and J. Weber, Phys. Rev. B **33**, 8892 (1986).
[7] Y. K. Kwon, T. Ishikawa, and H. Kuwano, J. Appl. Phys. **61**, 1055 (1987).
[8] A. A. Gill, N. Baber, and M. Z. Iqbal, J. Appl. Phys. **67**, 1130 (1990).
[9] R. B. Firestone and V. S. Shirley, *Table of Isotopes* (Wiley, New York, 1996).
[10] N. Achtziger, Mater. Sci. Forum **248-249**, 113 (1997).
[11] N. Achtziger, J. Grillenberger, and W. Witthuhn, Hyperfine Interact. **120/121**, 69 (1999).
[12] N. Achtziger, H. Gottschalk, T. Licht, J. Meier, U. Reislöhner, M. Rüb, and W. Witthuhn, Appl. Phys. Lett. **66**, 2370 (1995).
[13] J. P. Biersack and J. F. Ziegler, *The Stopping and Ranges of Ions in Matter* (Pergamon, New York, 1985),Vol. 1.
[14] S. Weiss and R. Kassing, Solid-State Electron. **31**, 1733 (1988).

[15] D. Pons, J. Appl. Phys. **55**, 3644 (1984).
[16] D. K. Schroder, *Semiconductor Material and Device Characterization* (Wiley-Interscience, New York, 1998).
[17] P. Blood and J. W. Orton, *The Electrical Characterization of Semiconductors: Majority Carriers and Electron States* (Academic, London, 1992).
[18] H. Metzner, R. Sielemann, R. Butt, and S. Klaumützer, Phys. Rev. Lett. **53**, 290 (1984).
[19] H. Metzner, R. Sielemann, S. Klaumützer, and H. Hunger, Mater. Sci. Forum **15-18**, 1063 (1987).
[20] R. Devanathan, F. Gao, and W. J. Weber, Appl. Phys. Lett. **84**, 3909 (2004).
[21] J. Grillenberger, R. Sielemann, U. Grossner, F. Albrecht, B. G. Svensson, and W. Witthuhn (unpublished).
[22] J. Grillenberger, N. Achtziger, R. Sielemann, and W. Witthuhn, J. Appl. Phys. **88**, 3260 (2000).
[23] T. Dalibor, Phys. Status Solidi A **162**, 199 (1997).
[24] J. P. Doyle, M. O. Aboelfotoh, and B. G. Svensson, Mater. Sci. Forum **264-268**, 565 (1998).
[25] A. A. Lebedev, Semiconductors **33**, 107 (1999).
[26] C. Hemmingsson, N. T. Son, O. Kordina, E. Janzén, J. L. Lindström, S. Savage, and N. Nordell, Mater. Sci. Eng., B **46**, 336 (1997).
[27] C. Hemmingsson, N. T. Son, O. Kordina, J. P. Bergman, J. L. Lindström, S. Savage, N. Nordell, and E. Janzén, J. Appl. Phys. **81**, 6155 (1997).